DESY 05-093
July 2005

ISSN 0418-9833

A Determination of Electroweak Parameters at HERA

H1 Collaboration

Abstract

Using the deep inelastic e^+p and e^-p charged and neutral current scattering cross sections previously published, a combined electroweak and QCD analysis is performed to determine electroweak parameters accounting for their correlation with parton distributions. The data used have been collected by the H1 experiment in 1994-2000 and correspond to an integrated luminosity of $117.2\,\mathrm{pb}^{-1}$. A measurement is obtained of the W propagator mass in charged current ep scattering. The weak mixing angle $\sin^2\theta_W$ is determined in the on-mass-shell renormalisation scheme. A first measurement at HERA is made of the light quark weak couplings to the Z^0 boson and a possible contribution of right-handed isospin components to the weak couplings is investigated.

(To be submitted to Phys. Lett. B.)

A. Aktas[10], V. Andreev[26], T. Anthonis[4], S. Aplin[10], A. Asmone[34], A. Astvatsatourov[4], A. Babaev[25], S. Backovic[31], J. Bähr[39], A. Baghdasaryan[38], P. Baranov[26], E. Barrelet[30], W. Bartel[10], S. Baudrand[28], S. Baumgartner[40], J. Becker[41], M. Beckingham[10], O. Behnke[13], O. Behrendt[7], A. Belousov[26], Ch. Berger[1], N. Berger[40], J.C. Bizot[28], M.-O. Boenig[7], V. Boudry[29], J. Bracinik[27], G. Brandt[13], V. Brisson[28], D.P. Brown[10], D. Bruncko[16], F.W. Büsser[11], A. Bunyatyan[12,38], G. Buschhorn[27], L. Bystritskaya[25], A.J. Campbell[10], S. Caron[1], F. Cassol-Brunner[22], K. Cerny[33], V. Cerny[16,47], V. Chekelian[27], J.G. Contreras[23], J.A. Coughlan[5], B.E. Cox[21], G. Cozzika[9], J. Cvach[32], J.B. Dainton[18], W.D. Dau[15], K. Daum[37,43], Y. de Boer[25], B. Delcourt[28], A. De Roeck[10,45], K. Desch[11], E.A. De Wolf[4], C. Diaconu[22], V. Dodonov[12], A. Dubak[31,46], G. Eckerlin[10], V. Efremenko[25], S. Egli[36], R. Eichler[36], F. Eisele[13], M. Ellerbrock[13], W. Erdmann[40], S. Essenov[25], A. Falkewicz[6], P.J.W. Faulkner[3], L. Favart[4], A. Fedotov[25], R. Felst[10], J. Ferencei[16], L. Finke[11], M. Fleischer[10], P. Fleischmann[10], Y.H. Fleming[10], G. Flucke[10], A. Fomenko[26], I. Foresti[41], G. Franke[10], T. Frisson[29], E. Gabathuler[18], E. Garutti[10], J. Gayler[10], C. Gerlich[13], S. Ghazaryan[38], S. Ginzburgskaya[25], A. Glazov[10], I. Glushkov[39], L. Goerlich[6], M. Goettlich[10], N. Gogitidze[26], S. Gorbounov[39], C. Goyon[22], C. Grab[40], T. Greenshaw[18], M. Gregori[19], B.R. Grell[10], G. Grindhammer[27], C. Gwilliam[21], D. Haidt[10], L. Hajduk[6], M. Hansson[20], G. Heinzelmann[11], R.C.W. Henderson[17], H. Henschel[39], O. Henshaw[3], G. Herrera[24], M. Hildebrandt[36], K.H. Hiller[39], D. Hoffmann[22], R. Horisberger[36], A. Hovhannisyan[38], T. Hreus[16], S. Hussain[19], M. Ibbotson[21], M. Ismail[21], M. Jacquet[28], L. Janauschek[27], X. Janssen[10], V. Jemanov[11], L. Jönsson[20], D.P. Johnson[4], A.W. Jung[14], H. Jung[20,10], M. Kapichine[8], J. Katzy[10], N. Keller[41], I.R. Kenyon[3], C. Kiesling[27], M. Klein[39], C. Kleinwort[10], T. Klimkovich[10], T. Kluge[10], G. Knies[10], A. Knutsson[20], V. Korbel[10], P. Kostka[39], K. Krastev[10], J. Kretzschmar[39], A. Kropivnitskaya[25], K. Krüger[14], J. Kückens[10], M.P.J. Landon[19], W. Lange[39], T. Laštovička[39,33], G. Laštovička-Medin[31], P. Laycock[18], A. Lebedev[26], G. Leibenguth[40], V. Lendermann[14], S. Levonian[10], L. Lindfeld[41], K. Lipka[39], A. Liptaj[27], B. List[40], E. Lobodzinska[39,6], N. Loktionova[26], R. Lopez-Fernandez[10], V. Lubimov[25], A.-I. Lucaci-Timoce[10], H. Lueders[11], D. Lüke[7,10], T. Lux[11], L. Lytkin[12], A. Makankine[8], N. Malden[21], E. Malinovski[26], S. Mangano[40], P. Marage[4], R. Marshall[21], M. Martisikova[10], H.-U. Martyn[1], S.J. Maxfield[18], D. Meer[40], A. Mehta[18], K. Meier[14], A.B. Meyer[11], H. Meyer[37], J. Meyer[10], S. Mikocki[6], I. Milcewicz-Mika[6], D. Milstead[18], D. Mladenov[35], A. Mohamed[18], F. Moreau[29], A. Morozov[8], J.V. Morris[5], M.U. Mozer[13], K. Müller[41], P. Murín[16,44], K. Nankov[35], B. Naroska[11], Th. Naumann[39], P.R. Newman[3], C. Niebuhr[10], A. Nikiforov[27], D. Nikitin[8], G. Nowak[6], M. Nozicka[33], R. Oganezov[38], B. Olivier[3], J.E. Olsson[10], S. Osman[20], D. Ozerov[25], V. Palichik[8], I. Panagoulias[10], T. Papadopoulou[10], C. Pascaud[28], G.D. Patel[18], M. Peez[29], E. Perez[9], D. Perez-Astudillo[23], A. Perieanu[10], A. Petrukhin[25], D. Pitzl[10], R. Plačakytė[27], B. Portheault[28], B. Povh[12], P. Prideaux[18], N. Raicevic[31], P. Reimer[32], A. Rimmer[18], C. Risler[10], E. Rizvi[19], P. Robmann[41], B. Roland[4], R. Roosen[4], A. Rostovtsev[25], Z. Rurikova[27], S. Rusakov[26], F. Salvaire[11], D.P.C. Sankey[5], E. Sauvan[22], S. Schätzel[10], F.-P. Schilling[10], S. Schmidt[10], S. Schmitt[10], C. Schmitz[41], L. Schoeffel[9], A. Schöning[40], H.-C. Schultz-Coulon[14], K. Sedlák[32], F. Sefkow[10], R.N. Shaw-West[3], I. Sheviakov[26], L.N. Shtarkov[26], T. Sloan[17], P. Smirnov[26], Y. Soloviev[26], D. South[10], V. Spaskov[8], A. Specka[29], B. Stella[34], J. Stiewe[14], I. Strauch[10], U. Straumann[41], V. Tchoulakov[8], G. Thompson[19], P.D. Thompson[3], F. Tomasz[14], D. Traynor[19], P. Truöl[41], I. Tsakov[35], G. Tsipolitis[10,42], I. Tsurin[10], J. Turnau[6], E. Tzamariudaki[27], M. Urban[41], A. Usik[26], D. Utkin[25], S. Valkár[33], A. Valkárová[33], C. Vallée[22], P. Van Mechelen[4], A. Vargas

Trevino[7], Y. Vazdik[26], C. Veelken[18], A. Vest[1], S. Vinokurova[10], V. Volchinski[38], B. Vujicic[27], K. Wacker[7], J. Wagner[10], G. Weber[11], R. Weber[40], D. Wegener[7], C. Werner[13], N. Werner[41], M. Wessels[10], B. Wessling[10], C. Wigmore[3], Ch. Wissing[7], R. Wolf[13], E. Wünsch[10], S. Xella[41], W. Yan[10], V. Yeganov[38], J. Žáček[33], J. Zálešák[32], Z. Zhang[28], A. Zhelezov[25], A. Zhokin[25], Y.C. Zhu[10], J. Zimmermann[27], T. Zimmermann[40], H. Zohrabyan[38] and F. Zomer[28]

[1] *I. Physikalisches Institut der RWTH, Aachen, Germany*[a]
[2] *III. Physikalisches Institut der RWTH, Aachen, Germany*[a]
[3] *School of Physics and Astronomy, University of Birmingham, Birmingham, UK*[b]
[4] *Inter-University Institute for High Energies ULB-VUB, Brussels; Universiteit Antwerpen, Antwerpen; Belgium*[c]
[5] *Rutherford Appleton Laboratory, Chilton, Didcot, UK*[b]
[6] *Institute for Nuclear Physics, Cracow, Poland*[d]
[7] *Institut für Physik, Universität Dortmund, Dortmund, Germany*[a]
[8] *Joint Institute for Nuclear Research, Dubna, Russia*
[9] *CEA, DSM/DAPNIA, CE-Saclay, Gif-sur-Yvette, France*
[10] *DESY, Hamburg, Germany*
[11] *Institut für Experimentalphysik, Universität Hamburg, Hamburg, Germany*[a]
[12] *Max-Planck-Institut für Kernphysik, Heidelberg, Germany*
[13] *Physikalisches Institut, Universität Heidelberg, Heidelberg, Germany*[a]
[14] *Kirchhoff-Institut für Physik, Universität Heidelberg, Heidelberg, Germany*[a]
[15] *Institut für Experimentelle und Angewandte Physik, Universität Kiel, Kiel, Germany*
[16] *Institute of Experimental Physics, Slovak Academy of Sciences, Košice, Slovak Republic*[f]
[17] *Department of Physics, University of Lancaster, Lancaster, UK*[b]
[18] *Department of Physics, University of Liverpool, Liverpool, UK*[b]
[19] *Queen Mary and Westfield College, London, UK*[b]
[20] *Physics Department, University of Lund, Lund, Sweden*[g]
[21] *Physics Department, University of Manchester, Manchester, UK*[b]
[22] *CPPM, CNRS/IN2P3 - Univ. Mediterranee, Marseille - France*
[23] *Departamento de Fisica Aplicada, CINVESTAV, Mérida, Yucatán, México*[k]
[24] *Departamento de Fisica, CINVESTAV, México*[k]
[25] *Institute for Theoretical and Experimental Physics, Moscow, Russia*[l]
[26] *Lebedev Physical Institute, Moscow, Russia*[e]
[27] *Max-Planck-Institut für Physik, München, Germany*
[28] *LAL, Université de Paris-Sud, IN2P3-CNRS, Orsay, France*
[29] *LLR, Ecole Polytechnique, IN2P3-CNRS, Palaiseau, France*
[30] *LPNHE, Universités Paris VI and VII, IN2P3-CNRS, Paris, France*
[31] *Faculty of Science, University of Montenegro, Podgorica, Serbia and Montenegro*[e]
[32] *Institute of Physics, Academy of Sciences of the Czech Republic, Praha, Czech Republic*[e,i]
[33] *Faculty of Mathematics and Physics, Charles University, Praha, Czech Republic*[e,i]
[34] *Dipartimento di Fisica Università di Roma Tre and INFN Roma 3, Roma, Italy*
[35] *Institute for Nuclear Research and Nuclear Energy, Sofia, Bulgaria*[e]
[36] *Paul Scherrer Institut, Villigen, Switzerland*
[37] *Fachbereich C, Universität Wuppertal, Wuppertal, Germany*
[38] *Yerevan Physics Institute, Yerevan, Armenia*
[39] *DESY, Zeuthen, Germany*

[40] *Institut für Teilchenphysik, ETH, Zürich, Switzerland*[j]
[41] *Physik-Institut der Universität Zürich, Zürich, Switzerland*[j]

[42] *Also at Physics Department, National Technical University, Zografou Campus, GR-15773 Athens, Greece*
[43] *Also at Rechenzentrum, Universität Wuppertal, Wuppertal, Germany*
[44] *Also at University of P.J. Šafárik, Košice, Slovak Republic*
[45] *Also at CERN, Geneva, Switzerland*
[46] *Also at Max-Planck-Institut für Physik, München, Germany*
[47] *Also at Comenius University, Bratislava, Slovak Republic*

[a] *Supported by the Bundesministerium für Bildung und Forschung, FRG, under contract numbers 05 H1 1GUA /1, 05 H1 1PAA /1, 05 H1 1PAB /9, 05 H1 1PEA /6, 05 H1 1VHA /7 and 05 H1 1VHB /5*
[b] *Supported by the UK Particle Physics and Astronomy Research Council, and formerly by the UK Science and Engineering Research Council*
[c] *Supported by FNRS-FWO-Vlaanderen, IISN-IIKW and IWT and by Interuniversity Attraction Poles Programme, Belgian Science Policy*
[d] *Partially Supported by the Polish State Committee for Scientific Research, SPUB/DESY/P003/DZ 118/2003/2005*
[e] *Supported by the Deutsche Forschungsgemeinschaft*
[f] *Supported by VEGA SR grant no. 2/4067/ 24*
[g] *Supported by the Swedish Natural Science Research Council*
[i] *Supported by the Ministry of Education of the Czech Republic under the projects INGO-LA116/2000 and LN00A006, by GAUK grant no 175/2000*
[j] *Supported by the Swiss National Science Foundation*
[k] *Supported by CONACYT, México, grant 400073-F*
[l] *Partially Supported by Russian Foundation for Basic Research, grant no. 00-15-96584*

1 Introduction

The deep inelastic scattering (DIS) of leptons off nucleons has played an important role in revealing the structure of matter, in the discovery of weak neutral current interactions and in the foundation of the Standard Model (SM) as the theory of strong and electroweak (EW) interactions. At HERA, the first lepton-proton collider ever built, the study of DIS has been pursued since 1992 over a wide kinematic range. In terms of Q^2, the negative four-momentum transfer squared, the kinematic coverage includes the region where the electromagnetic and weak interactions become of comparable strength. Both charged current (CC) and neutral current (NC) interactions occur in ep collisions and are studied by the two collider experiments H1 and ZEUS. Many QCD analyses of HERA data have been performed to determine the strong interaction coupling constant α_s [1–3] and parton distribution functions (PDFs) [2, 4, 5]. In EW analyses, the W boson mass value has been determined from the charged current data at high Q^2 [4, 6–11]. Previously the QCD and EW sectors were analysed independently.

Based solely on the precise data recently published by H1 [1, 4, 5, 8], a combined QCD and EW analysis is performed here for the first time and parameters of the electroweak theory are determined. The data have been taken by the H1 experiment in the first phase of operation of HERA (HERA-I) with unpolarised e^+ and e^- beams and correspond to an integrated luminosity of $100.8\,\mathrm{pb}^{-1}$ for e^+p and $16.4\,\mathrm{pb}^{-1}$ for e^-p respectively. A measurement is made of the W mass in the space-like region from the propagator mass (M_{prop}) in charged current scattering. The masses of the W boson (M_W) and top quark (m_t) and the weak mixing angle ($\sin^2\theta_W$) are determined within the electroweak $\mathrm{SU}(2)_L \times \mathrm{U}(1)_Y$ Standard Model. The vector and axial-vector weak couplings of the light (u and d) quarks to the Z^0 boson are measured for the first time at HERA. These results are complementary to determinations of EW parameters at LEP, the Tevatron and low energy experiments [12].

2 Charged and Neutral Current Cross Sections

2.1 Charged Current Cross Section

The charged current interactions, $e^\pm p \to (\overline{\nu}_e) X$, are mediated by the exchange of a W boson in the t channel. The measured cross section for unpolarised beams after correction for QED radiative effects [13–15] can be expressed as

$$\frac{d^2\sigma^{\mathrm{CC}}(e^\pm p)}{dxdQ^2} = \frac{G_F^2}{2\pi x}\left[\frac{M_W^2}{M_W^2+Q^2}\right]^2 \phi_{CC}^{\pm}(x,Q^2)\left(1+\Delta_{CC}^{\pm,weak}\right), \quad (1)$$

$$\text{with} \quad \phi_{CC}^{\pm}(x,Q^2) = \frac{1}{2}\left[Y_+ W_2^{\pm}(x,Q^2) \mp Y_- x W_3^{\pm}(x,Q^2) - y^2 W_L^{\pm}(x,Q^2)\right]. \quad (2)$$

Here G_F is the Fermi constant accounting for radiative corrections to the W propagator as measured in muon decays and $\Delta_{CC}^{\pm,weak}$ represents the other weak vertex and box corrections, which amount to a few per mil [16] and are neglected. The term $\phi_{CC}^{\pm}$ [4] contains the structure functions $W_2^{\pm}$, $xW_3^{\pm}$ and $W_L^{\pm}$. The factors $Y_\pm$ are defined as $Y_\pm = 1 \pm (1-y)^2$ and y is the

inelasticity variable which is related to Bjorken x, Q^2 and the centre-of-mass energy squared s by $y = Q^2/xs$.

Within the SM, the CC cross section in Eqn.(1) can be expressed in the so-called on-mass-shell (OMS) scheme [17] replacing the Fermi constant G_F with:

$$G_F = \frac{\pi\alpha}{\sqrt{2}M_W^2\left(1-\frac{M_W^2}{M_Z^2}\right)}\frac{1}{1-\Delta r}\,, \tag{3}$$

where $\alpha \equiv \alpha(Q^2=0)$ is the fine structure constant and M_Z is the mass of the Z^0 boson. The term Δr contains one-loop and leading higher-order EW radiative corrections. The one-loop contributions can be expressed as [16]

$$\Delta r = \Delta\alpha - \frac{\cos^2\theta_W}{\sin^2\theta_W}\Delta\rho + \Delta r_{\rm rem}\,. \tag{4}$$

The first term $\Delta\alpha$ is the fermionic part of the photon vacuum polarisation. It has a calculable leptonic contribution and an uncalculable hadronic component which can however be estimated using e^+e^- data [18]. Numerically these two contributions are of similar size and have a total value of 0.059 [19] when evaluated at M_Z^2. The quantity $\Delta\rho$ arises from the large mass difference between the top and bottom quarks in the vector boson self-energy loop:

$$\Delta\rho = \frac{3\alpha}{16\pi\sin^2\theta_W\cos^2\theta_W}\frac{m_t^2}{M_Z^2}\,, \tag{5}$$

after neglecting the mass of the bottom quark. The second term in Eqn.(4) has a numerical value of about 0.03. The last term $\Delta r_{\rm rem}$ is numerically smaller (~ 0.01). It contains the remaining contributions including those with logarithmic dependence on m_t and the Higgs boson mass M_H. Leading higher-order terms proportional to $G_F^2 m_t^4$ and $\alpha\alpha_s$ are included as well. In Eqns.(4,5) and the OMS scheme, it is understood that

$$\sin^2\theta_W = 1 - M_W^2/M_Z^2. \tag{6}$$

In the quark parton model (QPM), the structure functions $W_2^\pm$ and $xW_3^\pm$ may be interpreted as lepton charge dependent sums and differences of quark and anti-quark distributions and are given by

$$W_2^+ = x(\overline{U}+D),\quad xW_3^+ = x(D-\overline{U}),\quad W_2^- = x(U+\overline{D}),\quad xW_3^- = x(U-\overline{D})\,, \tag{7}$$

whereas $W_L^\pm = 0$. The terms xU, xD, $x\overline{U}$ and $x\overline{D}$ are defined as the sum of up-type, of down-type and of their anti-quark-type distributions, i.e. below the b quark mass threshold:

$$xU = x(u+c),\quad xD = x(d+s),\quad x\overline{U} = x(\overline{u}+\overline{c}),\quad x\overline{D} = x(\overline{d}+\overline{s})\,. \tag{8}$$

In next-to-leading-order (NLO) QCD and the $\overline{\rm MS}$ renormalisation scheme [20], these simple relations do not hold any longer and $W_L^\pm$ becomes non-zero. Nevertheless the capability of the CC cross sections to probe up- and down-type quarks remains.

2.2 Neutral Current Cross Section

The NC interactions, $e^{\pm}p \to e^{\pm}X$, are mediated by photon (γ) or Z^0 exchange in the t channel. The measured NC cross section with unpolarised beams after correction for QED radiative effects [13, 15, 21] is given by

$$\frac{d^2\sigma^{\rm NC}(e^{\pm}p)}{dxdQ^2} = \frac{2\pi\alpha^2}{xQ^4}\phi^{\pm}_{NC}(x,Q^2)\left(1+\Delta^{\pm,weak}_{NC}\right), \quad (9)$$

$$\text{with} \quad \phi^{\pm}_{NC}(x,Q^2) = Y_+\tilde{F}_2(x,Q^2) \mp Y_- x\tilde{F}_3(x,Q^2) - y^2\tilde{F}_L(x,Q^2), \quad (10)$$

where $\Delta^{\pm,weak}_{NC}$ represents weak radiative corrections which are typically less than 1% and never more than 3%. The NC structure function term $\phi^{\pm}_{NC}$ [4] is expressed in terms of the generalised structure functions $\tilde{F}_2$, $x\tilde{F}_3$ and $\tilde{F}_L$. The first two can be further decomposed as [22]

$$\tilde{F}_2 \equiv F_2 - v_e\frac{\kappa Q^2}{(Q^2+M_Z^2)}F_2^{\gamma Z} + (v_e^2+a_e^2)\left(\frac{\kappa Q^2}{Q^2+M_Z^2}\right)^2 F_2^Z, \quad (11)$$

$$x\tilde{F}_3 \equiv - a_e\frac{\kappa Q^2}{(Q^2+M_Z^2)}xF_3^{\gamma Z} + (2v_ea_e)\left(\frac{\kappa Q^2}{Q^2+M_Z^2}\right)^2 xF_3^Z. \quad (12)$$

Here

$$\kappa^{-1} = \frac{2\sqrt{2}\pi\alpha}{G_F M_Z^2}, \quad (13)$$

in the modified on-mass-shell (MOMS) scheme [23], in which all EW parameters can be defined in terms of α, G_F and M_Z (besides fermion masses and quark mixing angles), or

$$\kappa^{-1} = 4\frac{M_W^2}{M_Z^2}\left(1-\frac{M_W^2}{M_Z^2}\right)(1-\Delta r) \quad (14)$$

in the OMS scheme. The quantities v_e and a_e are the vector and axial-vector weak couplings of the electron to the Z^0 [12]. In the bulk of the HERA phase space, $\tilde{F}_2$ is dominated by the electromagnetic structure function F_2 originating from photon exchange only. The functions F_2^Z and xF_3^Z are the contributions to $\tilde{F}_2$ and $x\tilde{F}_3$ from Z^0 exchange and the functions $F_2^{\gamma Z}$ and $xF_3^{\gamma Z}$ are the contributions from γZ interference. These contributions only become important at large values of Q^2.

In the QPM, the longitudinal structure function $\tilde{F}_L$ equals zero and the structure functions F_2, $F_2^{\gamma Z}$ and F_2^Z are related to the sum of the quark and anti-quark momentum distributions, xq and $x\overline{q}$,

$$[F_2, F_2^{\gamma Z}, F_2^Z] = x\sum_q [e_q^2, 2e_qv_q, v_q^2+a_q^2]\{q+\overline{q}\}, \quad (15)$$

whereas the structure functions $xF_3^{\gamma Z}$ and xF_3^Z are related to their difference,

$$[xF_3^{\gamma Z}, xF_3^Z] = 2x\sum_q [e_qa_q, v_qa_q]\{q-\overline{q}\}. \quad (16)$$

In Eqns.(15,16) e_q is the electric charge of quark q, and v_q and a_q are, respectively, the vector and axial-vector weak coupling constants of the quarks to the Z^0:

$$v_q = I^3_{q,L} - 2e_q\sin^2\theta_W, \quad (17)$$

$$a_q = I^3_{q,L} \quad (18)$$

where $I^3_{q,L}$ is the third component of the weak isospin.

The weak radiative corrections $\Delta^{\pm,weak}_{NC}$ in Eqn.(9) correspond effectively to modifications of the weak neutral current couplings to so-called dressed couplings by four weak form factors ρ_{eq}, κ_e, κ_q and κ_{eq} [16]. The form factor ρ_{eq} has a numerical value very close to 1 for $Q^2 \lesssim 10\,000\,\mathrm{GeV}^2$ and only at very high Q^2 a deviation of a few percent is reached [16]. The form factors $\kappa_{e,q,eq}$ fall strongly with Q^2 [16] and approach unity where the γZ and Z^0 contributions become significant. Given the current precision of the data used (Section 3), in the following analysis $\rho_{eq} = 1$ is assumed and the weak mixing angle in Eqn.(17) is replaced by an effective one, $\sin^2\theta^{\mathrm{eff}}_W = \kappa_q(1 - M^2_W/M^2_Z)$, where κ_q is assumed to be flavour independent and equal to the universal part of the form factors [19].

3 Data Sets and Fit Strategies

The analysis performed here uses (as in [5]) the following H1 data sets: two low Q^2 data sets ($1.5 \leq Q^2 \leq 150\,\mathrm{GeV}^2$) [1], three high Q^2 NC data sets ($100 \leq Q^2 \leq 30\,000\,\mathrm{GeV}^2$) [4, 5, 8] and three high Q^2 CC data sets ($300 \leq Q^2 \leq 15\,000\,\mathrm{GeV}^2$) [4,5,8]. These data cover a Bjorken x range from $3 \cdot 10^{-5}$ to 0.65 depending on Q^2.

The low Q^2 data are dominated by systematic uncertainties which have a precision down to 2% in most of the covered region. The high Q^2 data on the other hand are mostly limited by the statistical precision which is up to 30% or larger for $Q^2 \gtrsim 10\,000\,\mathrm{GeV}^2$.

The combined EW-QCD analysis follows the same fit procedure as used in [5]. The QCD analysis is performed using the DGLAP evolution equations [24] at NLO [25] in the $\overline{\mathrm{MS}}$ renormalisation scheme. All quarks are taken to be massless.

Fits are performed to the measured cross sections assuming the strong coupling constant to be equal to $\alpha_s(M_Z) = 0.1185$. The analysis uses an x-space program developed within the H1 Collaboration [26]. In the fit procedure, a χ^2 function which is defined in [1] is minimised. The minimisation takes into account correlations between data points caused by systematic uncertainties [5].

In the fits, five PDFs – gluon, xU, xD, $x\overline{U}$ and $x\overline{D}$ – are defined by 10 free parameters as in [5]. Table 1 shows an overview of various fits that are performed in the present paper to determine different EW parameters. For all fits, the PDFs obtained here are consistent with those from the H1 PDF 2000 fit [5]. For more details refer to [27].

4 Results

4.1 Determination of Masses and $\sin^2\theta_W$

The cross section data allow a simultaneous determination of G_F and M_W and of the PDFs as independent parameters (fit G-M_{prop}-PDF in Table 1). In this fit, the parameters G_F and

Fit	Fixed parameters	
	CC	NC
G-$M_{\rm prop}$-PDF	$-$	α, G_F, M_Z
$M_{\rm prop}$-PDF	G_F	α, G_F, M_Z
M_W-PDF	α, M_Z, m_t, M_H	
m_t-PDF	α, M_Z, M_W, M_H	
v_u-a_u-v_d-a_d-PDF	G_F, M_W	α, M_Z, M_W
v_u-a_u-PDF	G_F, M_W	$\alpha, M_Z, M_W, v_d, a_d$
v_d-a_d-PDF	G_F, M_W	$\alpha, M_Z, M_W, v_u, a_u$
$I^3_{u,R}$-$I^3_{d,R}$-PDF	G_F, M_W	$\alpha, M_Z, M_W, v_{q,L}, a_{q,L}$

Table 1: Summary of the main fit assumptions. In the fits, in addition to the free parameters listed in the first column, the systematic correlation uncertainty parameters are allowed to vary (see Table 2 in [5]). The fixed parameters are set to values taken from [12] and M_H is set to 120 GeV.

M_W in Eqn.(1) are considered to be a normalisation variable G and a propagator mass $M_{\rm prop}$, respectively, independent of the SM. The sensitivity to G according to Eqn.(1) results from the normalisation of the CC cross section whereas the sensitivity to $M_{\rm prop}$ arises from the Q^2 dependence. The fit is performed including the NC cross section data in order to constrain the PDFs. The result of the fit to G and $M_{\rm prop}$ is shown in Fig. 1 as the shaded area. The χ^2 value per degree of freedom (dof) is $533.0/610 = 0.87$. The correlation between G and $M_{\rm prop}$ is -0.85, and is found to be larger than the correlations with the QCD parameters [28]. This determination of G is consistent with the more precise value of $1.16637 \cdot 10^{-5}\,{\rm GeV}^{-2}$ of G_F obtained from the muon lifetime measurement [12], demonstrating the universality of the CC interaction over a large range of Q^2 values.

Fixing G to G_F, one may fit the CC propagator mass $M_{\rm prop}$ only. For this fit ($M_{\rm prop}$-PDF), the EW parameters are defined in the MOMS scheme and the propagator mass $M_{\rm prop}$ is considered to be independent of any other EW parameters. Note that in the MOMS scheme, the use of G_F makes the dependency of the CC and NC cross sections on m_t and M_H negligibly small. The result of the fit, also shown in Fig. 1, is

$$M_{\rm prop} = 82.87 \pm 1.82_{\rm exp}\ ^{+0.30}_{-0.16}\big|_{\rm model}\ {\rm GeV}\,. \tag{19}$$

Here the first error is experimental and the second corresponds to uncertainties due to input parameters and model assumptions as introduced in Table 5 in [5] (e.g. the variation of $\alpha_s = 0.1185 \pm 0.0020$). The χ^2 value per dof is $533.3/611$. If the PDFs are fixed in the fit, the experimental error on $M_{\rm prop}$ is reduced to 1.5 GeV, which indicates that the correlation between $M_{\rm prop}$ and the QCD parameters is not very strong but not negligible either [27]. The determination given in Eqn.(19) represents the most accurate measurement so far of the CC propagator mass at HERA [4, 7–11].

The propagator mass $M_{\rm prop}$ measured here in the space-like region can be compared with direct W boson mass measurements obtained in the time-like region by the Tevatron and LEP experiments. The value is consistent with the world average of $M_W = 80.425 \pm 0.038$ GeV [12] within 1.3 standard deviations.

Within the SM, the CC and NC cross sections can be expressed in the OMS scheme in which all EW parameters are determined by α, M_Z and M_W together with m_t and M_H in the loop corrections. In this scheme, the CC cross section normalisation depends on M_W via the $G_F - M_W$ relation (Eqn.(3)). Some additional sensitivity to M_W comes through the M_W dependent terms (e.g., Eqn.(14)) in the NC cross section. Fixing m_t to its world average value of $178\,\mathrm{GeV}$ [12] and assuming $M_H = 120\,\mathrm{GeV}$, the fit M_W-PDF leads to

$$M_W = 80.786 \pm 0.205_{\mathrm{exp}}\,{}^{+0.048}_{-0.029}\big|_{\mathrm{model}} \pm 0.025_{\delta m_t} - 0.084_{\delta M_H} \pm 0.033_{\delta(\Delta r)}\,\mathrm{GeV}\,. \qquad (20)$$

Here, in addition to the experimental and model uncertainties, three other error sources are considered: the uncertainty on the top quark mass $\delta m_t = 4.3\,\mathrm{GeV}$ [12], a variation of the Higgs mass from $120\,\mathrm{GeV}$ to $300\,\mathrm{GeV}$ and the uncertainty of higher-order terms in Δr [27,29]. It should be pointed out that the result Eqn.(20) on M_W is not a direct measurement but an indirect SM parameter determination which provides a consistency check of the model.

Together with the world average value of $M_Z = 91.1876 \pm 0.0021\,\mathrm{GeV}$ [12], the result obtained on M_W from Eqn.(20) represents an indirect determination of $\sin^2\theta_W$ in the OMS scheme (Eqn.(6))

$$\sin^2\theta_W = 0.2151 \pm 0.0040_{\mathrm{exp}}\,{}^{+0.0019}_{-0.0011}\big|_{\mathrm{th}} \qquad (21)$$

where the first error is experimental and the second is theoretical covering all remaining uncertainties in Eqn.(20). The uncertainty due to δM_Z is negligible.

Fixing M_W to the world average value and assuming $M_H = 120\,\mathrm{GeV}$, the fit m_t-PDF gives $m_t = 108 \pm 44\,\mathrm{GeV}$ where the uncertainty is experimental. The result represents the first determination of the top quark mass through loop effects in the ep data at HERA.

4.2 Determination of $v_{u,d}$ and $a_{u,d}$

At HERA, the NC interactions at high Q^2 receive contributions from γZ interference and Z^0 exchange (Eqns.(15,16)). Thus the NC data can be used to extract the weak couplings of up- and down-type quarks to the Z^0 boson. At high Q^2 and high x, where the NC $e^{\pm}p$ cross sections are sensitive to these couplings, the up- and down-type quark distributions are dominated by the light u and d quarks. Therefore, this measurement can be considered to determine the light quark couplings. The CC cross section data help disentangle the up and down quark distributions.

In this analysis (fit v_u-a_u-v_d-a_d-PDF), the vector and axial-vector dressed couplings of u and d quarks are treated as free parameters. The results of the fit are shown in Fig. 2 and are given in Table 2. The effect of the u and d correlation is illustrated in Fig. 2 by fixing either u or d quark couplings to their SM values (fits v_d-a_d-PDF and v_u-a_u-PDF). The precision is better for the u quark as expected. The superior precision for a_u comes from the γZ interference contribution $xF_3^{\gamma Z}$ (Eqn.(16)). The d-quark couplings v_d and a_d are mainly constrained by the Z^0 exchange term F_2^Z (Eqn.(15)). These differences in sensitivity result in the different contour shapes shown in Fig. 2.

The results do not depend significantly on the low x data, nor on the assumptions on the parton distributions at low x where DGLAP may fail. This was checked by performing two

Fit	a_u	v_u	a_d	v_d	χ^2/dof
v_u-a_u-v_d-a_d-PDF	0.56 ± 0.10	0.05 ± 0.19	-0.77 ± 0.37	-0.50 ± 0.37	$531.7/608$
v_u-a_u-PDF	0.57 ± 0.08	0.27 ± 0.13	$-$	$-$	$534.1/610$
v_d-a_d-PDF	$-$	$-$	-0.80 ± 0.24	-0.33 ± 0.33	$532.6/610$
SM value	0.5	0.196	-0.5	-0.346	$-$

Table 2: The results of the fits to the weak neutral current couplings in comparison with their SM values. The correlation between the the fit parameters may be found in [30].

other fits, one for which the data at $x \leq 0.0005$ are excluded, and another one for which the normalisation constraint on the low x behaviour of the anti-quark distributions is relaxed[1]. This limited influence of the low x region on the values of the fitted EW couplings is partly due to the fact that electroweak effects are most prominent at large x and Q^2. Moreover the correlations between the fitted couplings and the PDF parameters are moderate, amounting to at most 21% [30].

The results from this analysis are also compared in Fig. 2 with similar results obtained recently by the CDF experiment [31]. The HERA determination has comparable precision to that from the Tevatron. These determinations are sensitive to u and d quarks separately, contrary to other measurements of the light quark-Z^0 couplings in νN scattering [32] and atomic parity violation [33] on heavy nuclei. They also resolve any sign ambiguity and the ambiguities between v_u and a_u of the determinations based on observables measured at the Z^0 resonance [34].

In more general EW models which consider other weak isospin multiplet structure, the vector and axial-vector couplings in Eqns.(17,18) are modified in the following way [35]

$$v_q = I^3_{q,L} + I^3_{q,R} - 2e_q\kappa_q \sin^2\theta_W \quad (22)$$

$$a_q = I^3_{q,L} - I^3_{q,R}\,. \quad (23)$$

Fixing $I^3_{q,L}$ and $\sin^2\theta_W$ to their SM values, a fit to $I^3_{u,R}$ and $I^3_{d,R}$ is performed (fit $I^3_{u,R}$-$I^3_{d,R}$-PDF). The results are shown in Fig. 3. Both quantities are consistent with the SM prediction $I^3_{q,R} = 0$, although the precision is not yet sufficient to exclude a contribution of quarks in right-handed multiplets.

5 Conclusion

Using the neutral and charged current cross section data recently published by H1, combined electroweak and QCD fits have been performed. In this analysis the correlation between the electroweak and parton distribution parameters is taken into account and a set of electroweak theory parameters is determined for the first time at HERA.

[1]Further relations between the QCD parameters are given by sum rules and thus were not relaxed. The number of parameters which determine the parton densities was unchanged with respect to the QCD fit performed in [5], where it was obtained using a well-defined χ^2 minimisation procedure.

Exploiting the Q^2 dependence of the charged current data, the propagator mass has been measured with the result $M_{\rm prop} = 82.87 \pm 1.82_{\rm exp}\ ^{+0.30}_{-0.16}\big|_{\rm model}\ {\rm GeV}$. Within the Standard Model framework, the W mass has been determined to be $M_W = 80.786 \pm 0.205_{\rm exp}\ ^{+0.063}_{-0.098}\big|_{\rm th}\ {\rm GeV}$ in the on-mass-shell scheme. This mass value has also been used to derive an indirect determination of $\sin^2\theta_W$ yielding $0.2151 \pm 0.0040_{\rm exp}\ ^{+0.0019}_{-0.0011}\big|_{\rm th}$. Furthermore, a result on the top quark mass via electroweak effects in ep data has been obtained.

The vector and axial-vector weak neutral current couplings of u and d quarks to the Z^0 boson have been determined at HERA for the first time. A possible contribution to the weak neutral current couplings from right-handed current couplings has also been studied. All results are consistent with the electroweak Standard Model.

Acknowledgements

We are grateful to the HERA machine group whose outstanding efforts have made this experiment possible. We thank the engineers and technicians for their work in constructing and maintaining the H1 detector, our funding agencies for financial support, the DESY technical staff for continual assistance and the DESY directorate for support and for the hospitality which they extend to the non DESY members of the collaboration. It is our pleasure to thank H. Spiesberger for helpful discussions.

References

[1] C. Adloff *et al.* [H1 Collaboration], Eur. Phys. J. **C21** (2001) 33 [hep-ex/0012053].

[2] S. Chekanov *et al.* [ZEUS Collaboration], Phys. Rev. **D67** (2003) 012007 [hep-ex/0208023].

[3] S. Chekanov *et al.* [ZEUS Collaboration], submitted to Eur. Phys. J. [hep-ph/0503274].

[4] C. Adloff *et al.* [H1 Collaboration], Eur. Phys. J. **C13** (2000) 609 [hep-ex/9908059].

[5] C. Adloff *et al.* [H1 Collaboration], Eur. Phys. J. **C30** (2003) 1 [hep-ex/0304003].

[6] T. Ahmed *et al.* [H1 Collaboration], Phys. Lett. B **324** (1994) 241.

[7] S. Aid *et al.* [H1 Collaboration], Phys. Lett. B **379** (1996) 319 [hep-ex/9603009].

[8] C. Adloff *et al.* [H1 Collaboration], Eur. Phys. J. **C19** (2001) 269 [hep-ex/0012052].

[9] J. Breitweg *et al.* [ZEUS Collaboration], Eur. Phys. J. **C12** (2000) 411 [hep-ex/9907010]; [Erratum ibid. **B27** (2003) 305].

[10] S. Chekanov *et al.* [ZEUS Collaboration], Phys. Lett. **B539** (2002) 197 [hep-ex/0205091]; [Erratum ibid. B **552** (2003) 308].

[11] S. Chekanov *et al.* [ZEUS Collaboration], Eur. Phys. J. **C32** (2003) 1 [hep-ex/0307043].

[12] S. Eidelman *et al.* [Particle Data Group Collaboration], Phys. Lett. **B592** (2004) 1.

[13] D. Y. Bardin, K. C. Burdik, P. K. Khristova and T. Riemann, Z. Phys. C **44** (1989) 149.

[14] M. Böhm and H. Spiesberger, Nucl. Phys. B **304** (1988) 749; H. Spiesberger, Nucl. Phys. B **349** (1991) 109.

[15] A. Kwiatkowski, H. Spiesberger and H. J. Möhring, Comput. Phys. Commun. **69** (1992) 155.

[16] W. Hollik *et al.*, Proceedings of the Workshop "Physics at HERA", vol.2, eds. W. Buchmüller and G. Ingelman, DESY (1992) 923.

[17] A. Sirlin, Phys. Rev. **D22** (1980) 971 and ibid. **D29** (1984) 89.

[18] See e.g., M. Davier, S. Eidelman, A. Höcker and Z. Zhang, Eur. Phys. J. **C27** (2003) 497 [hep-ph/0208177] and references therein.

[19] H. Spiesberger, http://www.desy.de/∼hspiesb/eprc.html.

[20] W. A. Bardeen, A. J. Buras, D. W. Duke and T. Muta, Phys. Rev. D **18** (1978) 3998.

[21] D. Y. Bardin, C. Burdik, P. C. Khristova and T. Riemann, Z. Phys. C **42** (1989) 679; M. Böhm and H. Spiesberger, Nucl. Phys. B **294** (1987) 1081; M. Böhm and H. Spiesberger, Nucl. Phys. B **304** (1988) 749.

[22] M. Klein and T. Riemann, Z. Phys. **C24** (1984) 151.

[23] W. F. L. Hollik, Fortschr. Phys. **38** (1990) 165.

[24] Y. L. Dokshitzer, Zh. Eksp. Teor. Fiz. **73** (1977) 1216 [Sov. Phys. JETP **46** (1977) 641]; V. N. Gribov and L. N. Lipatov, Yad. Fiz. **15** (1972) 1218 [Sov. J. Nucl. Phys. **15** (1972) 675]; V. N. Gribov and L. N. Lipatov, Yad. Fiz. **15** (1972) 781 [Sov. J. Nucl. Phys. **15** (1972) 438]; G. Altarelli and G. Parisi, Nucl. Phys. **B126** (1977) 298.

[25] W. Furmanski and R. Petronzio, Phys. Lett. **B97** (1980) 437.

[26] C. Pascaud and F. Zomer, LAL preprint, LAL 95-05 (1995);
C. Pascaud and F. Zomer, "A fast and precise method to solve the Altarelli-Parisi equations in x space" [hep-ph/0104013].

[27] B. Portheault, Ph.D. thesis (March 2005), LAL 05-05 (IN2P3/CNRS), Université de Paris Sud Orsay, available at http://www-h1.desy.de/publications/theses_list.html

[28] See http://www-h1.desy.de/psfiles/figures/d05-093.gf-mw.correlation for the uncertainties on the parameters and their correlations.

[29] B. A. Kniehl, Proceedings of the Workshop "Future Physics at HERA", vol.1, eds. G. Ingelman, A. De Roeck and R. Klanner DESY (1996) 160.

[30] See http://www-h1.desy.de/psfiles/figures/d05-093.vq-aq.correlation for the uncertainties on the parameters and their correlations.

[31] D. Acosta *et al.* [CDF Collaboration], Phys. Rev. D **71** (2005) 052002 [hep-ex/0411059].

[32] G. P. Zeller *et al.* [NuTeV Collaboration], Phys. Rev. Lett. **88** (2002) 091802 [hep-ex/0110059] [Erratum-ibid. **90** (2003) 239902].

[33] S. C. Bennett and C. E. Wieman, Phys. Rev. Lett. **82** (1999) 2484 [hep-ex/9903022].

[34] LEP and SLD Electroweak working groups, "A Combination of Preliminary Electroweak Measurements and Constraints on the Standard Model" [hep-ex/0412015]; http://lepewwg.web.cern.ch/LEPEWWG/plots/summer2004/.

[35] See e.g., M. Klein, T. Riemann and I. A. Savin, Phys. Lett. **B85** (1979) 385.

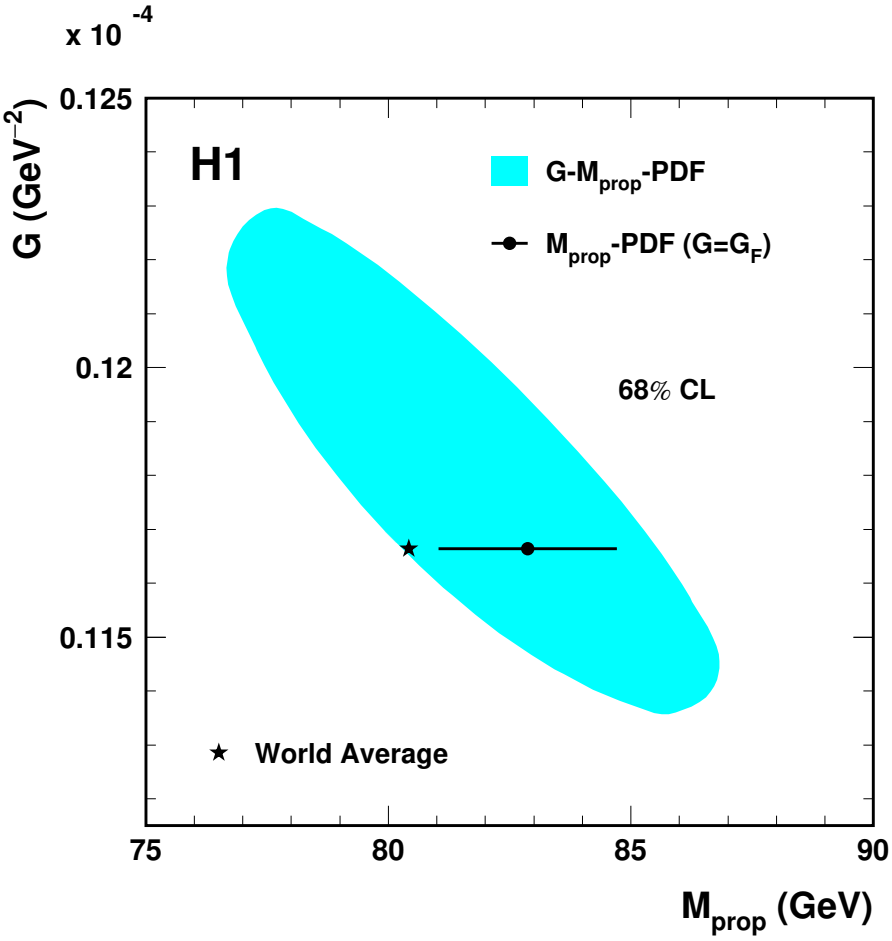

Figure 1: The result of the fit to G and $M_{\rm prop}$ at 68% confidence level (CL) shown as the shaded area. The world average values are indicated with the star symbol. Fixing G to G_F, the fit results in a measurement of the propagator mass $M_{\rm prop}$ shown as the circle with the horizontal error bars.

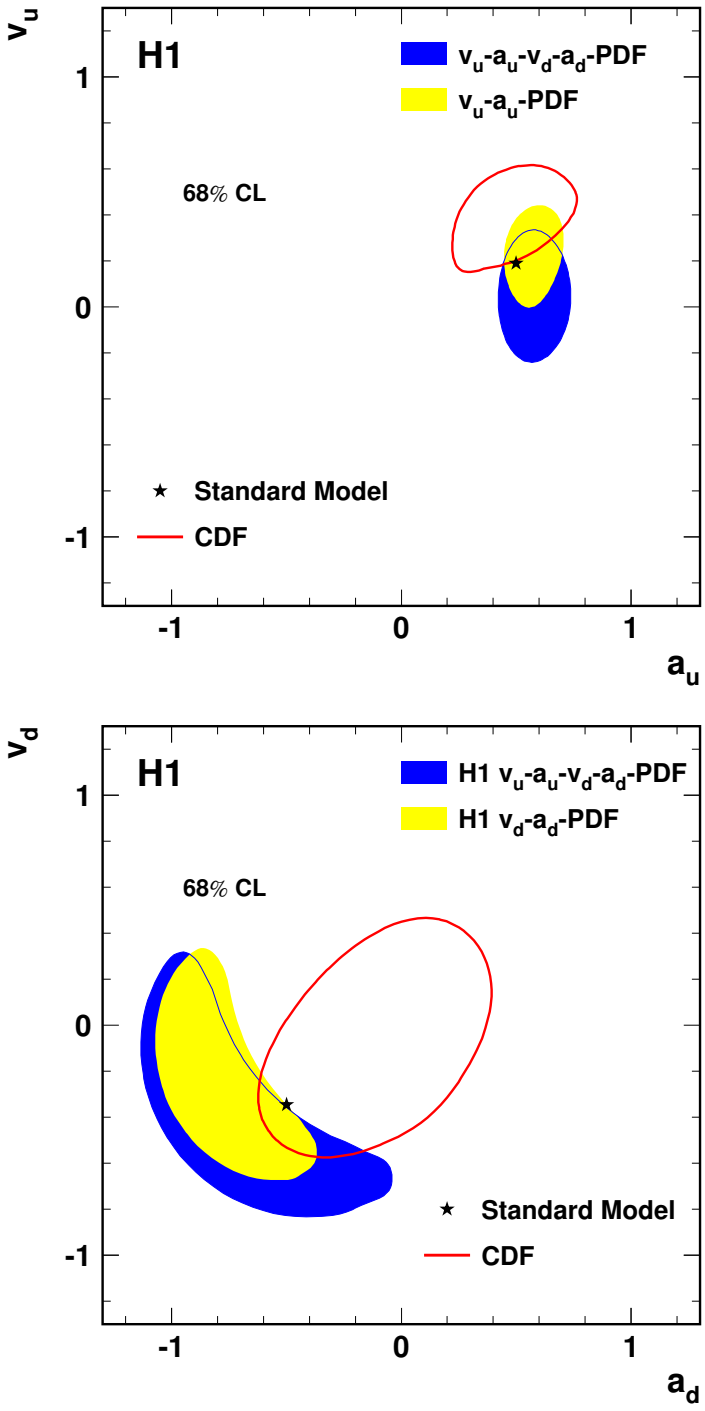

Figure 2: Results at 68% confidence level (CL) on the weak neutral current couplings of u (upper plot) and d (lower plot) quarks to the Z^0 boson determined in this analysis (shaded contours). The dark-shaded contours correspond to results of a simultaneous fit of all four couplings and can be compared with those determined by the CDF experiment (open contours). The light-shaded contours correspond to results of fits where either d or u quark couplings are fixed to their SM values. The stars show the expected SM values. Preliminary contours (not shown) obtained from e^+e^- measurements at the Z^0 resonance can be found in [34].

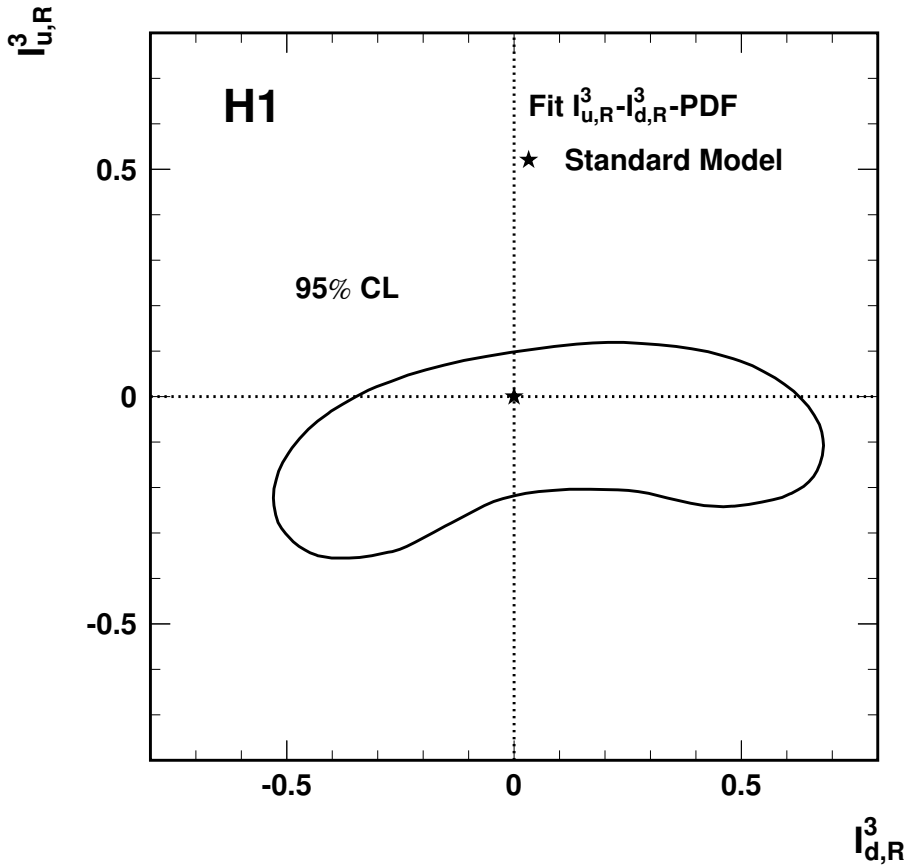

Figure 3: The result of the fit to the right-handed weak isospin charges $I^3_{u,R}$ and $I^3_{d,R}$ at 95% confidence level (CL). In the SM the right-handed charges are zero (star symbol).